ISSN 2075-1087, Gyroscopy and Navigation, 2018, Vol. 9, No. 4, pp. 267–276. © Pleiades Publishing, Ltd., 2018.
Published in Russian in Giroskopiya i Navigatsiya, 2018, No. 3, pp. 40–53.

Mathematical Analysis for the GPS Carrier Tracking Loop Phase Jitter in Presence of Different Types of Interference Signals

Ehab M. Shaheen*

Department of Electronic Warfare Military Technical College Cairo, Egypt

**e-mail: ehab.m.shaheen@mtc.edu.eg*

Received May 11, 2017

Abstract—The performance of a Global Positioning System (GPS) receiver usually depends on the tracking loops, so they can be considered the heart of the GPS receivers. It has been proven that the carrier tracking loop is more sensitive to noise and interference than the code tracking loop. Therefore, the carrier tracking loop can be used as a means for investigating the GPS receiver performance in presence of interference. In this paper, closed form analytical expressions for the carrier tracking loop phase error are derived in presence of different types of interference signals such as continuous wave interference, narrowband interference, partial band interference, broadband interference, match spectrum interference, and pulse interference. Also the carrier-to-noise ratio threshold is analytically derived. The derived analytical expressions have been validated with the aid of simulation experiments.

Keywords: GPS, NBI, carrier tracking loop, interference signals, carrier—to-noise ratio threshold

DOI: 10.1134/S2075108718040077

1. INTRODUCTION

The Doppler frequency and code delay parameters provided by the acquisition stage are not accurate enough to be used for positioning and navigation. Moreover, the phase information is ignored by the acquisition stage, and all these parameters are changing over time [1]. To this end, the tracking stage gives a fine estimate and dynamically follows the variations of the code delay, the Doppler frequency and the carrier phase [2]. A standard tracking process consists of two concatenated tracking loops. These tracking loops are used for tracking both the code delay and the carrier frequency. They are called code and carrier tracking loops.

The performance of a GPS receiver usually depends on the tracking loop, which enables continually the generation of the carrier and the code replicas that achieve maximum correlation in the receiver [2]. Only reliable signal tracking allows a GPS receiver to calculate the pseudo ranges and to extract the navigation data. In the case that the tacking loop cannot track the incoming GPS satellite signal, the position cannot be calculated [1].

The interference effect on the tracking loops has already been addressed by many researchers. In [3], the interference thresholds for a GPS receiver were obtained by a navigation laboratory test without any analytical analysis. In [4], the performance of the tracking loop under interference and dynamic effect was assessed by using software GPS receiver without any analytical analysis. In [5], the continuous wave interference (CWI) effect on the tracking performance of the GPS receivers was analyzed without investigating the parameters such as the carrier-to-noise ratio threshold, the GPS receiver interference tolerance, and the mean time to loss lock (MTLL).

The main objectives of this paper can be summarized as follows:

• to derive closed form analytical expressions for the carrier tracking loop phase jitter in presence of different most expected types of interference signals such as: continuous wave interference (CWI), narrowband interference (NBI), partial band interference (PBI), broadband interference (BBI), match spectrum interference (MSI) and pulse interference (PUI);

• to validate the derived analytical formulas with the aid of extensive simulation experiments.

This paper is organized as follows. The interference effect on the carrier tracking loop is measured by investigating the tracking loop phase jitter in section 2. A set of analytical and simulation results for different interference and GPS tracking loop parameters are presented in section 3. In section 4, the most efficient interference signal on a GPS receiver tracking loops is presented. Section 5 concludes the paper.

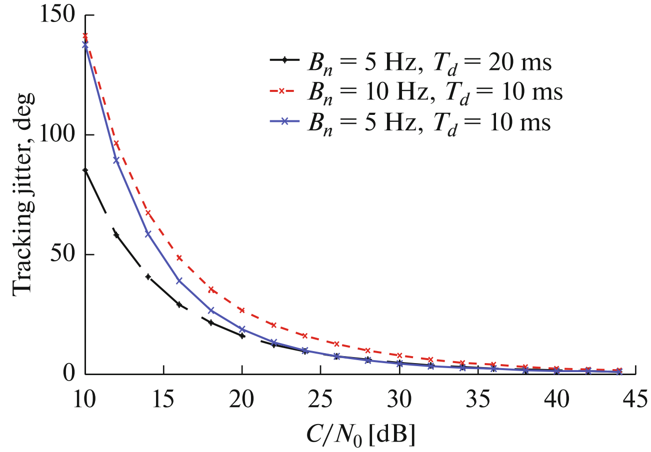

Fig. 1. Carrier tracking jitter at various C/N_0.

2. SYSTEM MODEL INTERFERENCE EFFECT ON THE CARRIER TRACKING LOOP PHASE JITTER

When comparing the carrier tracking loop to the code tracking loop, it can be noted that the carrier wavelength is much shorter than the code chip length, and the carrier loop needs to track all the dynamics while the code loop needs only to track the dynamic difference between the carrier loop and the code loop when carrier aiding is applied to the code loop [6]. Therefore, the carrier tracking loop is more sensitive to noise and interference than the code tracking loop. Thus, the carrier tracking loop can be used to investigate the GPS receiver performance in addition to the interference effect on the carrier tracking loop which can be measured by investigating the tracking loop phase jitter.

The carrier tracking loop phase jitter from all uncorrelated phase error sources can be written as [1]

$$\sigma_{\text{pll}} = \sqrt{\sigma_{\text{tp}}^2 + \sigma_{\text{v}}^2 + \sigma_{\text{A}}^2} + \frac{\theta_{\text{e}}}{3}, \tag{1}$$

where σ_{pll} is the tracking loop phase jitter, σ_{tp} is the thermal noise phase jitter, σ_{v} is the vibration-induced oscillator jitter in degrees, σ_{A} is the Allan deviation-induced oscillator jitter, and θ_{e} is the dynamic stress error.

The thermal noise phase jitter is written as [1]

$$\sigma_{\text{tp}} = \frac{180}{\pi}\sqrt{\frac{B_n}{C/N_0}\left(1 + \frac{1}{2T_d\, C/N_0}\right)}, \tag{2}$$

where B_n is the loop noise bandwidth (Hz), C/N_0 is the post-correlation carrier-to-noise density ratio, and T_d is the correlator coherent integration time.

For stationary or slow moving receiver, the effect of dynamic stress can be negligible, and the oscillator phase noise is small and transient. Without loss of generality, other sources of phase jittering can be neglected, and the thermal noise is considered as the only source for phase jittering.

Thus, the carrier tracking loop phase jitter σ_{pll} can be considered equal to the thermal noise jitter, and it can be written as

$$\sigma_{\text{pll}} = \sigma_{\text{tp}} = \frac{180}{\pi}\sqrt{\frac{B_n}{C/N_0}\left(1 + \frac{1}{2T_d\, C/N_0}\right)}. \tag{3}$$

Figure 1 depicts the phase jitter value for the carrier tracking loop at different values of coherent integration time T_d and noise bandwidth. It is shown that the carrier tracking loop phase jitter is strictly dependent on the noise bandwidth B_n, and the integration time T_d. In order to increase the performance of the carrier tracking loop in absence of interference, the coherent integration time can be increased or the carrier tracking loop noise bandwidth can be decreased.

For simple evaluation of the tracking loop in presence of interference, the following will be assumed:

1. The replica reference code is perfectly aligned with the satellite code $\tau_n = \tau_s = 0$.

2. The phase error $\Delta\theta$ is relatively constant over the integration period T_d.

The interference signal raises the noise power density in the correlator output causing a drop in the C/N_0 value. In [7], [8] and [9], the post-correlation C/N_0 for the GPS L1 coarse acquisition (C/A) code signal in presence of CWI, NBI, PBI, BBI, MSI or PUI [10] was analytically derived. Modifications can be done to these derived formulas in order to analyze the GPS receiver carrier tracking loop performances in presence of different interference signals.

The post-correlation C/N_0 in presence of CWI assesses the impact of CWI on the GPS receiver performance and can be written as [9]

$$\left(\frac{C}{N_0}\right)_{\text{CWI}} = \frac{P_s\left(1-\frac{|\Delta\tau|}{T_a}\right)^2 (\operatorname{sinc}(\pi\Delta f_D T_D))^2}{N_0 + T_D P_j |\acute{c}_w|^2 (\operatorname{sinc}(\pi\delta f_j T_D))^2}, \quad (4)$$

where Δf_D and $\Delta\tau$ are the carrier frequency estimation error and the code phase estimation error, respectively P_s is the GPS signal, P_j is the CWI power at the correlator input, $|\acute{c}_w|$ is the amplitude of the C/A code spectral-line number w and δf_j is the difference between the interference frequency and the nearest spectral line in the C/A code spectrum.

Note that the CWI effect on a GPS receiver corresponds to the amplitude of the nearest C/A code spectral line. The C/A code spectrum has a strong spectral line called the worst line.

Substituting into the carrier tracking phase jitter presented in equation (3), when the code phase estimation error $\Delta\tau = 0$; the tracking phase jitter in presence of CWI can be written as

$$\sigma_{\text{pll}} = \frac{180}{\pi}\sqrt{\frac{B_n\left(N_0 + T_d K P_j |\acute{c}_w|^2 (\operatorname{sinc}(\pi\delta f_j T_d))^2\right)}{K P_s (\operatorname{sinc}(\pi\Delta f_D T_d))^2}\left(1+\frac{N_0 + T_d K P_j |\acute{c}_w|^2 (\operatorname{sinc}(\pi\delta f_j T_d))^2}{2T_d K P_s (\operatorname{sinc}(\pi\Delta f_D T_d))^2}\right)}, \quad (5)$$

where the interference frequency error Δf_j is the difference between the interference frequency f_j and the receiver reference carrier frequency $\left(\Delta f_j = f_j - \hat{f}_D\right)$ and the non-coherent integration time $K = 1$.

For the evaluation of the derived mathematical expression for the tracking phase jitter in presence of CWI, comparison with the results presented in [5] will be achieved.

The tracking phase jitter in presence of CWI can be written as [5]

$$\sigma_{\text{pll}} = \frac{180}{\pi}\sqrt{B_n(1-0.5B_nT_d)\frac{\int_{-B/2}^{B/2} G_s(f)\,df + \frac{P_j}{N_0}T_d\operatorname{sinc}^2(\pi(f_j - w\Delta f)T_d)|\acute{c}_w|^2 S(w)}{\frac{C_s}{N_0}\left(\int_{-B/2}^{B/2} G_s(f)\,df\right)^2}\left(1+\frac{\int_{-B/2}^{B/2} G_s(f)\,df + \frac{P_j}{N_0}T_d\operatorname{sinc}^2(\pi(f_j - w\Delta f)T_d)|\acute{c}_w|^2 S(w)}{2T_d\frac{P_s}{N_0}\left(\int_{-B/2}^{B/2} G_s(f)\,df\right)^2}\right)}. \quad (6)$$

In [5], the GPS C/A code PRN6 was used, and it could be seen that the worst line component is at 227 kHz frequency with respect to the center frequency.

Comparison between the carrier tracking loop phase jitter in presence of CWI signal which was derived in the mathematical expression presented in equation (4) and the results presented in [5] is depicted in Fig. 1a and Fig. 2b when the integration time is equal to 5 and 20 ms respectively. In the case that the interference frequency varies from 255 to 299 kHz, the interference-to-signal power ratio $P_j/P_s = 8\,\text{dB}$, and the noise bandwidth of the carrier tracking loops is $B_n = 20\,\text{Hz}$. It can be noted that the results in [5] and the derived mathematical expression (5) results are in a good match.

In [5], the impact of CWI was only investigated. Due to the good match between the derived formula and the one presented in [5], following the same procedure, the tracking phase jitter in presence of different types of interference signals can be derived.

The post correlation C/N_0 in presence of NBI can be presented as [9]

$$\left(\frac{C}{N_0}\right)_{\text{NBI}} = \frac{P_s\left(1-\frac{|\Delta\tau|}{T_a}\right)^2 (\operatorname{sinc}(\pi\Delta f_D T_D))^2}{N_0 + \frac{P_j|\acute{c}_w|^2}{B_N}\sum_{\beta=-B_N T_D/2}^{B_N T_D/2}\left(\operatorname{sinc}\left(\pi\left(\delta f_j + \frac{\beta}{T_D}\right)T_D\right)\right)^2}. \quad (7)$$

Thus, the tracking phase jitter in presence of NBI can be formulated as

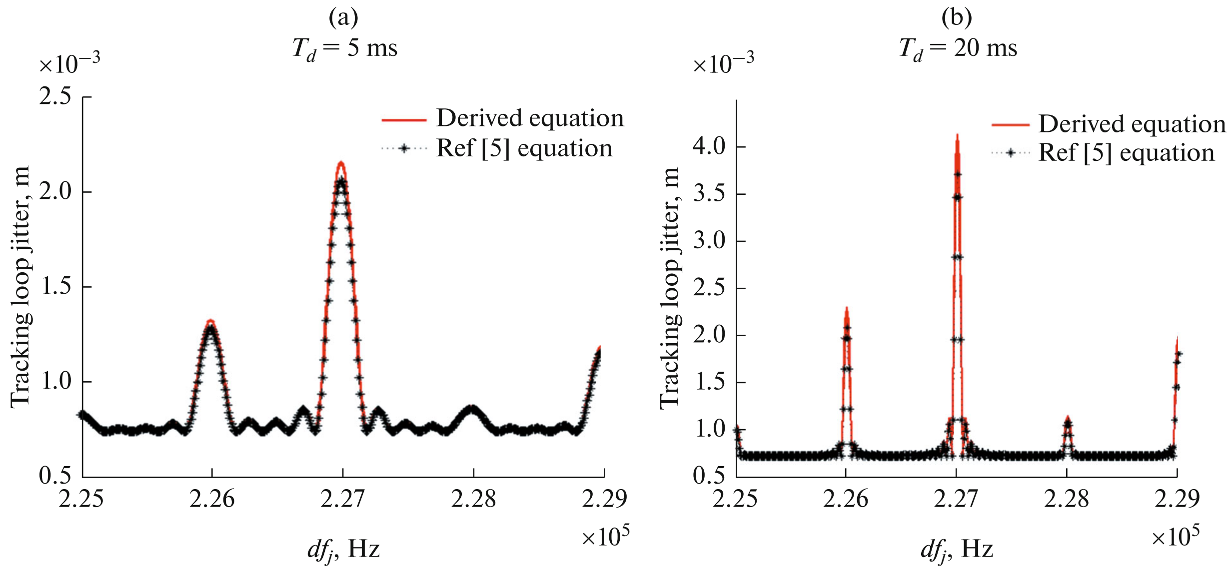

Fig. 2. Comparison between the new derived carrier tracking loop phase jitter and the one presented in [5].

$$\sigma_{\mathrm{pll}} = \frac{180}{\pi}\sqrt{\frac{B_n\left(N_0 + \frac{P_j K |\acute{c}_w|^2}{B_N}\sum_{\beta=-B_N\frac{T_d}{2}}^{B_N\frac{T_d}{2}}\left(\mathrm{sinc}\left(\pi\left(\delta f_j + \frac{\beta}{T_d}\right)T_d\right)\right)^2\right)}{P_s K\left(\mathrm{sinc}\left(\pi\Delta f_D T_d\right)\right)^2}\left(1 + \frac{N_0 + \frac{P_j K |\acute{c}_w|^2}{B_N}\sum_{\beta=-B_N T_d/2}^{B_N T_d/2}\left(\mathrm{sinc}\left(\pi\left(\delta f_j + \frac{\beta}{T_d}\right)T_d\right)\right)^2}{2T_d P_s K\left(\mathrm{sinc}\left(\pi\Delta f_D T_d\right)\right)^2}\right)}, \quad (8)$$

where N_j is the NBI power density, $N_j = P_j/B_N T_d$, P_j, is the NBI power at the correlator input and B_N is the interference bandwidth.

According to [9], the post correlation C/N_0 in presence of PBI can be written as

$$\left(\frac{C}{N_0}\right)_{\mathrm{PBI}} = \frac{P_s\left(1 - \frac{|\Delta\tau|}{T_a}\right)^2\left(\mathrm{sinc}\left(\pi\Delta f_D T_D\right)\right)^2}{N_0 + \frac{P_j}{B_N}\sum_{i=-B_N T_c/2}^{B_N T_c/2}\frac{T_a}{T_c}\left(\mathrm{sinc}\left(\pi\left(\frac{i}{T_c} - \Delta f_j\right)T_a\right)\right)^2}. \quad (9)$$

It was shown in [9] that the PBI power at the correlator output corresponds to the PSD of the PRN, which is covered by the PBI. It can be concluded that the PBI power at the correlator output is decreased by increasing the integration time. Thus, the PBI causes a drop in C/N_0 value.

Then, substituting in (3), the tracking phase jitter in presence of PBI can be formulated as

$$\sigma_{\text{pll}} = \frac{180}{\pi}\sqrt{\frac{B_n\left(N_0 + \frac{P_jK}{B_N}\sum_{i=-B_N\frac{T_c}{2}}^{+B_N\frac{T_c}{2}}\frac{T_a}{T_c}\left(\operatorname{sinc}\left(\pi\left(\frac{i}{T_c}-\Delta f_j\right)T_a\right)\right)^2\right)}{P_sK\left(\operatorname{sinc}\left(\pi\Delta f_DT_d\right)\right)^2} \left(\frac{B_n\left(N_0 + \frac{P_jK}{B_N}\sum_{i=-B_N\frac{T_c}{2}}^{+B_N\frac{T_c}{2}}\frac{T_a}{T_c}\left(\operatorname{sinc}\left(\pi\left(\frac{i}{T_c}-\Delta f_j\right)T_a\right)\right)^2\right)}{P_sK\left(\operatorname{sinc}\left(\pi\Delta f_DT_d\right)\right)^2}\right)}, \tag{10}$$

where T_a and T_c are the C/A code chip duration and period, respectively.

The post correlation C/N_0 in presence of BBI can be written as [9]

$$\left(\frac{C}{N_0}\right)_{\text{BBI}} = \frac{P_s\left(1-\frac{|\Delta\tau|}{T_a}\right)^2\left(\operatorname{sinc}\left(\pi\Delta f_DT_D\right)\right)^2}{N_0 + \frac{P_j}{B_N}}. \tag{11}$$

It was proven in [9] that the BBI power at correlator output corresponds only to the value of the correlator integration time and the interference bandwidth.

Then, by substituting in (3), the tracking phase jitter in presence of BBI can be formulated as

$$\sigma_{\text{pll}} = \frac{180}{\pi}\sqrt{\frac{B_n\left(N_0 + \frac{KP_j}{B_N}\right)}{P_sK\left(\operatorname{sinc}\left(\pi\Delta f_DT_d\right)\right)^2}\left(1 + \frac{N_0 + \frac{KP_j}{B_N}}{P_sK\left(\operatorname{sinc}\left(\pi\Delta f_DT_d\right)\right)^2}\right)}. \tag{12}$$

The post correlation C/N_0 in presence of MSI can be written as [7]

$$\left(\frac{C}{N_0}\right)_{\text{MSI}} = \frac{P_s\left[R_a(\tau_n)\operatorname{sinc}\left(2\pi\Delta f_DN_s\right)^2\right]}{N_0 + P_j\left|\grave{g}_w\right|^2\left(\operatorname{sinc}\left(\pi\delta f_jN_s\right)\right)^2}, \tag{13}$$

where $|\grave{g}_w|$ is the amplitude of the cross correlation sequence (CCS) Fourier series coefficient $\grave{g}$.

It was shown in [7] that, when the MSI spectral lines cross the GPS signal spectral lines, there are drops in the C/N_0; the drop of a C/N_0 value is mainly dependent on the amplitude of the CCS spectral line number.

The MSI has an effect on the GPS receiver performance only when the difference between the MSI spectral lines and the GPS signal spectral lines is less than the reciprocal of the integration time.

Then, by substituting in (3), the tracking phase jitter in presence of MSI can be formulated as

$$\sigma_{\text{pll}} = \frac{180}{\pi} \times \sqrt{\frac{B_n\left(N_0 + T_dKP_j\left|\grave{g}_w\right|^2\left(\operatorname{sinc}\left(\pi\delta f_jT_d\right)\right)^2\right)}{P_sK\left(\operatorname{sinc}\left(\pi\Delta f_DT_d\right)\right)^2}\left(1 + \frac{N_0 + T_dKP_j\left|\grave{g}_w\right|^2\left(\operatorname{sinc}\left(\pi\delta f_jT_d\right)\right)^2}{2T_dP_sK\left(\operatorname{sinc}\left(\pi\Delta f_DT_d\right)\right)^2}\right)}. \tag{14}$$

It was presented in [10] that the post correlation C/N_0 in presence of PUI can be written as

$$\left(\frac{C}{N_0}\right)_{\text{PUI}} = \frac{P_sK\left[R_a(\Delta\tau)\operatorname{sinc}\left(\pi\Delta f_DT_d\right)^2\right]}{N_0 + T_dP_jK\left|\sum_{i=-N_c}^{N_c}\sum_{s=-N_u}^{N_u}\acute{u}_s\acute{c}_ie^{j2\pi(\tau_n/T_c)i}\operatorname{sinc}\left(\pi\left[\frac{i}{T_c}+\frac{w}{T_c}+\frac{s}{T_p}+\delta f_j\right]T_d\right)\right|^2}, \tag{15}$$

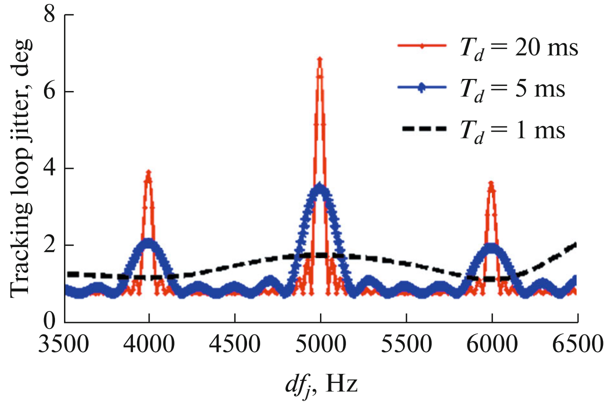

Fig. 3. CPJ in presence of CWI at different T_d values.

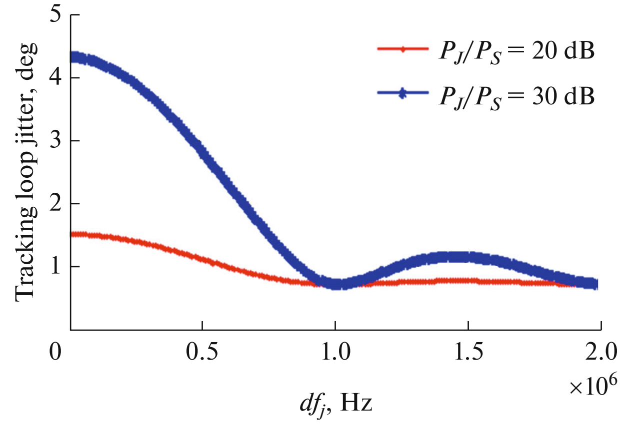

Fig. 5. CPJ in presence of PBI at different P_j/P_s values.

where $\acute{u}_s$ is the pulse sequence Fourier series coefficient, and T_p is the pulse period.

It was shown in [10] that the interference raises the noise floor in the correlator output causing a drop in the C/N_0 value.

By substituting in (3), the tracking phase jitter in presence of PUI can be formulated as

$$\sigma_{\text{pll}} = \frac{180}{\pi}\sqrt{\frac{B_n\left(N_0 + T_d P_j K\left|\sum_{i=-N_c}^{N_c}\sum_{s=-N_u}^{N_u}\acute{u}_s\acute{c}_i \operatorname{sinc}\left(\pi\left[\frac{i}{T_c}+\frac{w}{T_c}+\frac{s}{T_p}+\delta f_j\right]T_d\right)\right|^2\right)}{P_s\left(\operatorname{sinc}\left(\pi\Delta f_D T_d\right)\right)^2}\left(1+\frac{N_0 + T_d P_j K\left|\sum_{i=-N_c}^{N_c}\sum_{s=-N_u}^{N_u}\acute{u}_s\acute{c}_i \operatorname{sinc}\left(\pi\left[\frac{i}{T_c}+\frac{w}{T_c}+\frac{s}{T_p}+\delta f_j\right]T_d\right)\right|^2}{2T_d P_s\left(\operatorname{sinc}\left(\pi\Delta f_D T_d\right)\right)^2}\right)}. \quad (16)$$

In Fig. 3, the carrier phase jitter (CPJ) in presence of CWI signal versus the interference frequency error is depicted for interference-to-signal power ratio $P_j/P_s = 20\,\text{dB}$, and the noise bandwidth of the carrier tracking loops is $B_n = 5\,\text{Hz}$. This is done for different

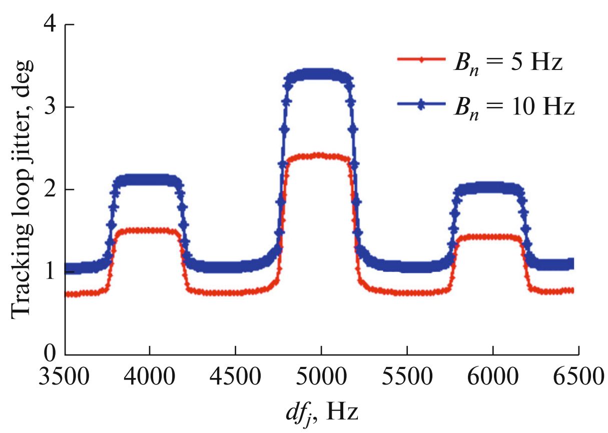

Fig. 4. CPJ in presence of NBI at different B_n values.

integration time values: 1, 5 and 20 ms. The amplitude of C/A code spectral line number zero is equal to zero. Thus, the interference frequency error range was chosen to be away from the zero spectral line, in order to avoid confusion in the analytical results. The interference frequency error Δf_j is assumed to vary from 3.5 to 6.5 kHz with 10 Hz step. It can be seen that the CWI can affect the carrier loop if its frequency is close to the C/A spectral line. Increasing the integration time, will increase the carrier tracking loop error. It can also be seen that the attenuation of the carrier tracking loop performance has similar characteristics as obtained for the C/N_0.

Figure 4 depicts the CPJ in presence of NBI signal with bandwidth 400 Hz, when P_j/P_s = 20 dB and the coherent integration equals to 20 ms. The noise bandwidth of the carrier tracking loops takes two values B_n = 5 and 10 Hz. It has been shown that the CPJ in presence of NBI is less than CPJ in the presence of CWI. When the B_n value is increased, the carrier tracking loop phase error will increase, too.

Figure 5 depicts the CPJ in presence of PBI signal with bandwidth B_N = 40 kHz; the interference frequency error varies from 0 to 2 MHz when P_j/P_s takes two values: 20 and 30 dB; and T_d = 20 ms. It has been shown that the PBI causes small jitter on the carrier tracking loop in comparison with the CWI or NBI, and its effect decreases by increasing the interference frequency error.

In Fig. 6, the CPJ in presence of BBI signal is depicted for P_j/P_s = 20 dB, and B_n = 5 Hz. This is done when the T_d = 20 ms. It has been shown that the effect of the BBI on the carrier loop decreases by increasing the BBI bandwidth.

In Fig. 7, the CPJ in presence of MSI is depicted when P_j/P_s = 20 dB. The integration time takes three values: 1, 5 and 20 ms. It has been shown that when the MSI spectral-lines cross the GPS signal spectral lines (which occur every 1 kHz), there is significant tracking loop phase jitter. The MSI can affect the carrier loop corresponding to the amplitude of the cross correlation sequence (CCS) spectral lines. Increasing the integration time will increase the carrier tracking loop error.

In Fig. 8, the CPJ in presence of PUI signal is depicted when P_j/P_s = 20 dB and $T_p = 10T_c$. The integration time takes two values: 5 and 20 ms. It has been shown that by increasing the coherent integration time, the carrier tracking loop phase jitter will increase.

It is worth noting that the mathematical formula in (3) which describes the CPJ is correct only in the linear region of the loop discriminator when the C/N_0 is greater than a specific threshold [6].

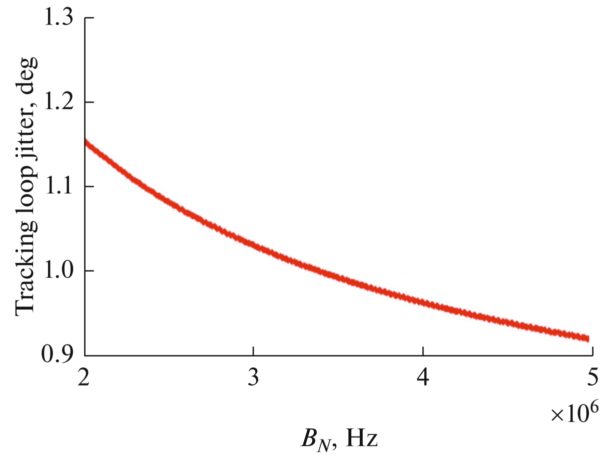

Fig. 6. CPJ in presence of BBI.

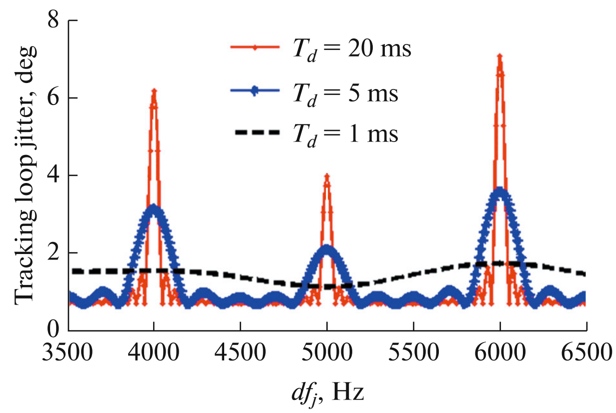

Fig. 7. CPJ in presence of MSI at different T_d values.

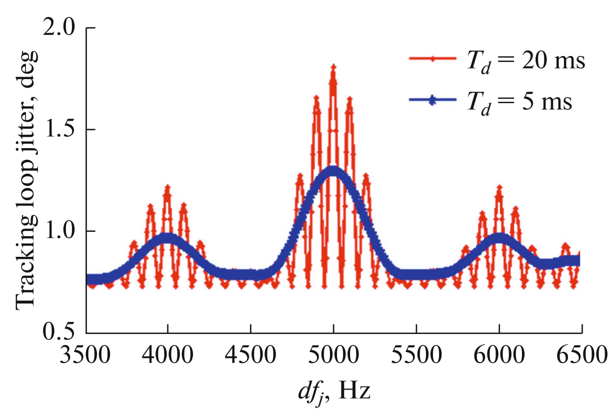

Fig. 8. CPJ in presence of PUI at different T_d values.

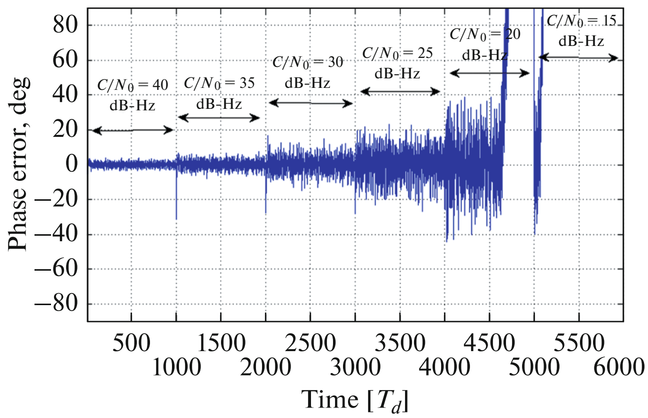

Fig. 9. The carrier tracking phase error at various C/N_0 values.

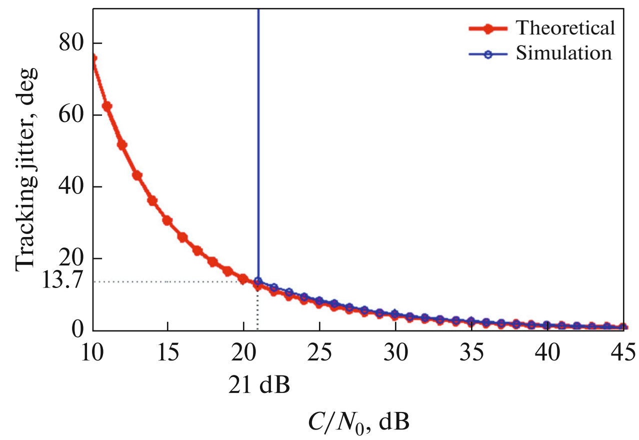

Fig. 10. Comparison of theoretical and simulated carrier tracking jitter.

For an unaided GPS receiver, the tracking threshold is typically set by the carrier tracking loop. However, when a receiver is aided with Doppler measurements from an Inertial Navigation System (INS), the tracking threshold will be determined by the code loop [2]. This is because Doppler aiding allows the numerical controlled oscillator to continue tracking the frequency of the desired signal, even when the carrier loop has been forced to lose lock.

In the following analysis, the receiver is assumed to be unaided, and the carrier-to-noise ratio threshold is assumed to be determined by the carrier loop.

The carrier-to-noise ratio threshold is defined as the minimum required C/N_0 at the correlator output, sufficient to maintain a stable lock with tracking error variance lower than a specific threshold [11]. The tracking loop exhibits the characteristic that, if the tracking error exceeds a certain boundary threshold, the tracking loop will no longer be able to track the signal and will lose the lock [2]. This is because the characteristics of the carrier tracking loop discriminators are nonlinear, especially near the threshold regions [5]. A conservative rule of thumb for tracking loop is that the 3-sigma phase jitter must not exceed 1/4 of the phase pull-in range of the carrier tracking loop discriminator [1]:

$$3\sigma_{\text{pll}} \le \alpha/4, \tag{17}$$

where α is the phase pull-in range.

By substituting (3) into (11), we obtain

$$\frac{\alpha}{12} = \frac{180}{\pi}\sqrt{\frac{B_n}{[C/N_0]_{\text{th}}}\left(1 + \frac{1}{2T_d\,[C/N_0]_{\text{th}}}\right)}, \tag{18}$$

where $[C/N_0]_{\text{th}}$ is the carrier-to-noise ratio threshold. The receiver is unable to keep track of signals if the post-correlation C/N_0 decreases below that threshold.

From (12) the $[C/N_0]_{\text{th}}$ can be derived as

$$[C/N_0]_{\text{th}} = \frac{B_n + \sqrt{B_n^2 + 2\gamma B_n/T_d}}{2\gamma}, \quad \gamma = \left(\frac{\alpha\pi}{2160}\right)^2. \tag{19}$$

The phase pull-in range of a Costas (the arctangent discriminator) loop discriminator is equal to $\pm\pi$, whereas a pure PLL discriminator has a pull-in range of $\pm 2\pi$ [1]. For the case where there is data modulation, the Costas loop is used. Therefore the Costas loop cannot tolerate phase jitter greater than 15° during the total dwell time [12].

The $[C/N_0]_{\text{th}}$ in case of Costas loop can be written as

$$[C/N_0]_{\text{th}} = \frac{B_n + \sqrt{B_n^2 + 0.1370\,B_n/T_d}}{0.1370}. \tag{20}$$

From (14) it can be seen that the carrier-to-noise ratio threshold is decreased by decreasing the loop noise bandwidth or increasing the integration time.

3. SIMULATION AND NUMERICAL RESULTS

This section introduces a simulation model for the third order Costas carrier tracking loop, with noise bandwidth of carrier tracking loops $B_n = 5\,\text{Hz}$, and the damping ratio was set to 0.707. The coherent integration time takes the values from 1 to 20 ms; the noncoherent integration value is fixed to $K = 1$. For fair comparison, the code phase estimate error is set to

$\Delta\tau = 0$, and the reference code in the GPS receiver is PRN1.

The tracking loop phase error is estimated at different carrier-to-noise ratios in order to investigate the carrier-to-noise ratio threshold.

In Fig. 9 the carrier loop phase error is estimated at different C/N_0 values (from 15 to 40 dB-Hz) by using the simulation model, during ($6000T_d = 120$ s), when $T_d = 20$ ms.

It should be noted that the loop rate equals to $f_L = 1/T_d = f_s/N_s$. Thus, the loop output phase error will be estimated once every integration time. By decreasing the C/N_0 value, the tracking phase error is increased and the tracking loop remains capable of tracking the signal until the C/N_0 value is less than a specific threshold (20 dB), after which the tracking loop suffers from the loss of lock on the input signal.

Figure 10 depicts the analytical and simulation carrier tracking jitter at various C/N_0 values (10 to 45 dB), in order to compare the simulation and analytical results using equation (3), and to determine the value of $[C/N_0]_{\mathrm{th}}$. It shows the agreement between the simulation and analytical results. The gap between the analytical and simulation results broadens suddenly and becomes very large when the phase jitter approaches a certain value; after this value the tracking loop enters the non-linear state and the linear assumption becomes invalid. The vertical trend in the curve computed from the simulation tracking error indicates that the loop has lost the lock. This phenomenon is not predicted by the theoretical jitter model (3) and (14) which is based on linear approximation of the loop. Also, it was found that the simulation value of the carrier-to-noise ratio threshold $[C/N_0]_{\mathrm{th}} = 21.4$ dB when the phase jitter equals to 13.7°. Yet, it follows analytically from formula (14) that $[C/N_0]_{\mathrm{th}} = 20.5$ dB when the phase jitter equals to 15° (that gives a good agreement between the simulation and analytical results).

4. CONCLUSIONS

In this paper, closed form analytical expressions for the carrier tracking loop phase error in presence of different interference signals were derived. The carrier-to-noise ratio threshold was analytically derived. The derived analytical expressions were validated with the aid of extensive simulation results.

It was shown that when the difference between the interference frequency and the nearest C/A spectral line was smaller than the reciprocal of the integration time, the CWI had a significant effect on the GPS receiver. In such a case, the CWI tolerance had a low value and the CWI tolerance value was proportional to the C/A code spectral line amplitude. At the same time, when this difference was greater than the reciprocal of the integration time, the CWI needed a relatively high power to affect the GPS receiver performance.

It was also found that, when the CWI frequency was coincident with the worst C/A line, A 20 dB CWI power above the GPS signal was sufficient to cause the loss of carrier lock. In NBI case, the interference tolerance value increased to 29 dB. For the case of PBI with the bandwidth equal to 5 kHz and the interference power by 38.5 dB more than the GPS signal power, the GPS carrier tracking loop lost the lock. Furthermore, for BBI, the tolerance value was 43.1 dB when its bandwidth $B_N = 2$ MHz. Finally, in the case when the MSI frequency was coincident with the worst CCS spectral line (number 226), the MSI tolerance value was nearly equal to that of CWI (only in the case when the CWI frequency was coincident with the C/A worst line). Also, it was shown that, when the MSI power was above the GPS signal by 20 dB, it was sufficient to cause the loss of lock in the GPS receiver.

REFERENCES

1. Kaplan, E.D. and Hegarty, C.J., Eds., *Understanding GPS Principles and Applications*, Artech House, 2006.
2. Parkinson, B. W. and Spilker, J. J., Eds., *Global Positioning System: Theory and Applications*, Washington DC: American Institute of Aeronautics and Astronautics, Inc, 1996.
3. Bakker, P. F. d., Effects of radio frequency interference on GNSS receiver output, *Master's Thesis*, Faculty of Aerospace Engineering, Delft University of Technology, 2006.
4. Kamel, A. M. M., Context aware high dynamics GNSS-INS for interference mitigation, *PhD Thesis*, Department of Geomatics Engineering, University of Calgary, 2011.
5. Jang, J., Paonni, M. and Eissfeller, B., CW Interference effects on tracking performance of GNSS receivers, *IEEE Transactions on Aerospace and Electronic Systems*, 2012, vol. 48(1), pp. 243–258.
6. Storm van Leeuwen, S., *Electromagnetic Interference on Low Cost GPS Receivers*, Amsterdam: National Aerospace Laboratory NLR, 2008.
7. Bek, M. K., Shaheen, E. M. and Elgamel, S. A., Evaluation of the GPS carrier to noise ratio in the presence of different interference signals, *IJAIEM*, 2013, vol. 2, pp. 458–468.
8. Bek, M. K., Shaheen, E. M. and Elgamel, S. A., Study of interference effects on the GPS receiver correlator, *Proc. ICEENG-9,* Cairo, Egypt, 2014.

9. Bek, M. K., Shaheen, E. M. and Elgamel, S. A., Classification and mathematical expression of different interference signals on the GPS receiver, *Journal of the Institute of Navigation,* 2015, vol. 62, no. 1, pp. 23–37.
10. Bek, M. K., Shaheen, E. M. and Elgamel, S. A., Mathematical analyses of pulse interference signal on post-correlation carrier-to-noise ratio for the global positioning system receivers, *IET Journal Radar, Sonar and Navigation,* 2015, vol. 9, no. 3, pp. 266–275.
11. Borio, D., Anantharamu, P. B and Lachapelle, G., Semi-analytic simulations: an extension to unambiguous BOC tracking, *Proc. International Technical Meeting of the Institute of Navigation,* San Diego, CA, 2010, pp. 1–14.
12. Razavi, A., Gebre-Egziabher, D. and Akos, D. M., Carrier loop architectures for tracking weak GPS signals, *IEEE Transactions on Aerospace and Electronic Systems,* 2008, vol. 44, no. 2, pp. 697–710.